




Neutron stars in a conservative $f(R, T)$ gravity

Ronaldo V. Lobato ¹, Geanderson A. Carvalho ^{2,3,4}, Carlos E. C. Montaña ⁵, and Jose F. Rodriguez-Ruiz ⁶

¹*Centro Brasileiro de Pesquisas Físicas, Rua Dr. Xavier Sigaud 150, Rio de Janeiro 22290-180, RJ, Brazil*

²*Departamento de Física, Universidade Tecnológica Federal do Paraná, Medianeira, PR, Brazil*

³*Programa de Pós-Graduação em Física e Astronomia,*

Universidade Tecnológica Federal do Paraná, Jardim das Américas 82590-300, Curitiba, PR, Brazil

⁴*Núcleo de Astrofísica e Cosmologia (Cosmo-Ufes), Universidade Federal do Espírito Santo,*

Av. Fernando Ferrari 514, Vitória, 29075-910, ES, Brazil

⁵*Facultad de Ciencias Básicas, Universidad Santiago de Cali,
Calle 5 62-00, Pampalinda, Cali, Valle del Cauca, Colombia*

⁶*Departamento de Física, Universidad Antonio Nariño,
Cra 3 Este # 47A - 15, Bogotá D.C. 110231, Colombia*

(Dated: May 12, 2026)

We investigate a conservative formulation of $f(R, T)$ gravity motivated by a key limitation of several existing approaches: the gravitational function is often reconstructed from a chosen equation of state, making the gravity sector EoS-dependent and compromising universality. To avoid this problem, we reformulate the theory in terms of an effective energy-momentum tensor, so that the conservation law follows from the field equations and Bianchi identities while the gravitational action remains independent of the microphysical EoS. We derive the modified stellar structure equations, establish theoretical consistency conditions including coupling bounds and crust-singularity avoidance, and present the tidal perturbation sector in terms of effective thermodynamic variables and an effective sound speed. We then compute neutron star observables using realistic tabulated EoSs, including mass-radius relations and tidal deformabilities, and compare the model with current astrophysical constraints from massive pulsars, NICER radius measurements, and GW170817.

I. INTRODUCTION

Understanding the behavior of matter and gravity under extreme conditions is a central goal of modern astrophysics. Compact objects such as neutron stars provide a unique laboratory for probing the properties of dense matter and testing gravitational theories in the strong-field regime. Observations of massive pulsars with masses close to two solar masses [1–4], together with radius measurements from the NICER mission [5–8] and tidal deformability constraints from gravitational wave observations of binary neutron star mergers [9], have significantly improved our ability to test both the microphysics of dense matter and the underlying theory of gravity.

General Relativity has been remarkably successful in describing gravitational phenomena over a wide range of scales. Nevertheless, theoretical and observational motivations continue to drive the exploration of modified theories of gravity [10–12]. Neutron stars are particularly powerful probes of such modifications in the strong-field regime [13–17]. Among these alternatives, $f(R)$ gravity and its extensions have attracted considerable attention. A particularly interesting generalization is the $f(R, T)$ theory of gravity, originally proposed by Harko *et al.* [18], in which the gravitational action depends not only on the Ricci scalar R but also on the trace T of the energy-momentum tensor. The trace dependent terms can be interpreted as an effective coupling between matter and geometry, which may arise from quantum effects [19] or from the presence of imperfect fluids [20].

A generic feature of $f(R, T)$ gravity is that the covariant divergence of the energy-momentum tensor does not vanish in general, $\nabla_\mu T^{\mu\nu} \neq 0$ [18, 21], reflecting the nonminimal coupling between matter and curvature. This feature has motivated the development of conservative formulations in which one instead imposes $\nabla_\mu T^{\mu\nu} = 0$. In particular, it has been proposed that this condition can be used to determine the functional form of $h(T)$ in models of the type $f(R, T) = R + h(T)$ [22]. Such formulations have been explored in both cosmological and astrophysical settings, including neutron stars [23, 24] and strange quark stars [25].

A conceptual difficulty with several energy-momentum conserving formulations of $f(R, T)$ gravity is that the functional form of the gravitational action is obtained by solving the conservation condition for a specific equation of state. In these approaches, the function $h(T)$ in models of the form $f(R, T) = R + h(T)$ is determined by combining the conservation equation with a chosen relation between pressure and energy density, such as a barotropic equation of state $p = \omega\rho$, a polytropic model $p = K\rho^\Gamma$, or the MIT bag model used to describe strange quark matter. The same conceptual issue arises for all these parameterizations. In barotropic models, changing ω changes the stiffness and therefore the reconstructed $h(T)$; in polytropic models, different choices of (K, Γ) play the same role; and in MIT bag descriptions, varying B (and ω , when treated as free) likewise changes the inferred $h(T)$. Thus, even when these EoSs are used as effective representations of uncertain microphysics, the reconstructed gravity function tracks modeling choices rather than a unique underlying theory.

In this situation, the gravitational Lagrangian becomes dependent on the microphysical properties of matter, effectively reversing the usual hierarchy in which the gravitational theory should be specified independently of the material sector. From this perspective, the result is not a unique modification of gravity but rather a family of theories associated with different equations of state.

This issue becomes particularly relevant in the modeling of neutron stars. Realistic nuclear equations of state encode a substantial amount of microphysical information about dense matter [26], including nuclear many-body interactions, three-body forces, the density dependence of the symmetry energy, and possible phase transitions to hyperonic or quark matter. Moreover, physically viable equations of state must satisfy theoretical constraints such as causality. In particular, the sound speed must obey $c_s^2 = dp/d\rho \leq 1$, ensuring that perturbations propagate at subluminal speeds [27, 28].

Modern neutron star equations of state are therefore obtained from microscopic nuclear calculations and are often implemented in tabulated form. If the gravitational action were determined from the equation of state, each nuclear model would correspond to a different gravitational theory. In such a scenario, modifying the nuclear interaction model or the high-density behavior of the equation of state would effectively modify the underlying theory of gravity. This creates a degeneracy between gravitational effects and uncertainties in the nuclear microphysics (e.g., [29]), making it difficult to disentangle genuine modifications of gravity from variations in the equation of state. Similar degeneracies have been discussed in the context of scalar-tensor and other modified gravity theories [30–33].

A further conceptual difficulty concerns the universality of the gravitational interaction. In metric theories of gravity, the form of the gravitational action is universal and does not depend on the particular properties of the matter configuration under consideration. If the functional form of $f(R, T)$ depends on the equation of state, then the gravitational theory would effectively change when different astrophysical systems are studied. For example, neutron stars described by nuclear equations of state, strange quark stars described by the MIT bag model, and cosmological fluids characterized by different equations of state would correspond to different gravitational Lagrangians.

This lack of universality is closely related to the Einstein equivalence principle, which states that the outcome of local non-gravitational experiments is independent of the composition and internal structure of matter. If the gravitational dynamics depend explicitly on the equation of state, then the gravitational interaction would effectively depend on the microscopic properties of the fluid describing the system, blurring the distinction between modifications of gravity and changes in the microphysical description of matter.

Motivated by these considerations, we investigate a formulation of $f(R, T)$ gravity in which the gravitational

action is specified independently of the equation of state and the trace dependent contributions are interpreted in terms of an effective energy-momentum tensor. In this approach, the conservation law emerges naturally from the field equations through the Bianchi identities, without imposing additional constraints that relate the gravitational Lagrangian to the microphysical properties of matter.

We apply this formulation to compact stars and derive the corresponding stellar structure equations. Using realistic neutron star equations of state obtained from nuclear many-body calculations, we investigate the impact of the modified gravity terms on the mass-radius relation and on the tidal properties of neutron stars. In particular, tidal deformability, which plays a central role in the gravitational-wave signal from binary neutron star mergers, provides an important observational probe of deviations from General Relativity. By solving the stellar structure equations together with the differential equation governing the tidal Love number, we compute the mass-radius relations and tidal deformabilities predicted by the model and compare them with current astrophysical constraints from massive pulsars [1, 2], NICER measurements [5, 6], and gravitational-wave observations such as GW170817.

II. CONSERVATIVE $f(R, T)$ MODELS

Several works in the literature attempt to construct energy-momentum conserved versions of $f(R, T)$ gravity by imposing the condition

$$\nabla_\mu T^{\mu\nu} = 0 \quad (1)$$

directly on the field equations in order to determine the functional form of the trace dependent function $h(T)$ in models of the form

$$f(R, T) = R + h(T). \quad (2)$$

In these approaches the conservation condition is solved simultaneously with a specific equation of state (EoS) describing the matter sector. For example, assuming a barotropic equation of state

$$p = \omega\rho \quad (3)$$

leads to a differential equation for $h_T = dh/dT$. The conservation equation is

$$(\rho + p) \frac{d}{dr} \ln h_T + \frac{1}{2} \frac{d}{dr} (\rho + 3p) = 0, \quad (4)$$

so

$$\frac{d \ln h_T}{d\rho} = -\frac{1 + 3\omega}{2(1 + \omega)} \frac{1}{\rho} \Rightarrow h_T(\rho) \propto \rho^{-\frac{1+3\omega}{2(1+\omega)}}. \quad (5)$$

Using $T = \rho - 3p = (1 - 3\omega)\rho$ (for $\omega \neq 1/3$), one has

$$h_T(T) = \frac{dh}{dT} \propto T^{-\frac{1+3\omega}{2(1+\omega)}}, \quad (6)$$

$$h(T) \propto T^{\frac{1-\omega}{2(1+\omega)}}. \quad (7)$$

where $\omega \neq -1$ is also required.

If a different equation of state is adopted, such as the MIT bag model for strange quark matter,

$$p = \omega(\rho - 4B), \quad (8)$$

a different functional form of $h(T)$ is obtained.

For the realistic nuclear EoSs, the conservation condition, Eq. (4), fixes $h_T(\rho)$ and therefore $h(T)$. In practice, the reconstructed function depends on the chosen matter model, i.e. $h(T) \equiv h(\rho, p(\rho))$, so the action is effectively

$$f(R, T) = R + h(\rho, p(\rho)). \quad (9)$$

Thus, the gravity sector becomes explicitly EoS-dependent. If one uses a database such as COMPOSE [34], which contains hundreds of models, one effectively obtains hundreds of gravity models.

This introduces a structural degeneracy in compact-star modeling: both EoS stiffness and the reconstructed gravity correction modify the same observables (mass-radius curves and tidal deformabilities). Since $h(T)$ is built from the EoS itself, part of what appears as a gravity signal can be reabsorbed into matter modeling, and vice versa. This leads to the following:

a. Non-uniqueness of the gravitational action For the class $f(R, T) = R + h(T)$, imposing $\nabla_\mu T^{\mu\nu} = 0$ after choosing an EoS does not compare different matter sectors within one fixed gravity theory. Instead, each EoS choice (barotropic, polytropic, MIT bag, or realistic tabulated nuclear EoS) generates a different reconstructed $h(T)$ and therefore a different effective Lagrangian.

b. Implications for neutron star inference In neutron star applications this mapping is particularly limiting, because realistic EoSs form families constrained by nuclear theory and observations rather than a unique input. As a consequence, varying EoS stiffness and varying gravity are not independent operations, which weakens direct interpretability of gravity constraints extracted from astrophysical data.

c. Universality and equivalence-principle motivation A fundamental gravity model should be defined once and then applied across systems (neutron stars, strange stars, cosmology) without changing the action. If $h(T)$ is reconstructed separately for each EoS class, this universality is blurred, and the effective dynamics acquires composition-dependent modeling choices from the matter sector.

These issues motivate the strategy adopted here: we specify the gravitational action a priori and absorb the trace dependent terms into an effective energy-momentum tensor,

$$G_{\mu\nu} = 8\pi T_{\mu\nu}^{\text{eff}}. \quad (10)$$

Then, from the Bianchi identity

$$\nabla_\mu G^{\mu\nu} = 0, \quad (11)$$

we obtain automatically

$$\nabla_\mu T^{\text{eff}\mu\nu} = 0. \quad (12)$$

In this formulation the EoS enters only at the level of matter closure in stellar-structure calculations, not in the definition of the gravity theory. This preserves a single gravitational framework while keeping the gravity-EoS degeneracy explicit and testable.

III. AN EFFECTIVE ENERGY-MOMENTUM TENSOR CONSERVATIVE $f(R, T)$ MODEL

A. Action and Field Equations

We consider the model $f(R, T) = R + 2\chi T$ [18], where R is the Ricci scalar, T is the trace of the energy-momentum tensor, and χ is a constant coupling parameter. For this model, the gravitational action is

$$S = \int \left[\frac{R + 2\chi T}{16\pi} + L_m \right] \sqrt{-g} d^4x, \quad (13)$$

where L_m is the matter Lagrangian density.

Assuming the standard perfect-fluid choice $L_m = -p$ and varying with respect to the metric yields

$$G_{\mu\nu} = 8\pi T_{\mu\nu} + 2\chi(T_{\mu\nu} + pg_{\mu\nu}) + \chi T g_{\mu\nu}. \quad (14)$$

For the perfect fluid, with $u^\mu u_\mu = 1$,

$$T_{\mu\nu} = (\rho + p)u_\mu u_\nu - pg_{\mu\nu}, \quad (15)$$

and

$$T = \rho - 3p. \quad (16)$$

B. Effective Energy-Momentum Tensor

The field equations can be rewritten as

$$G_{\mu\nu} = 8\pi T_{\mu\nu}^{\text{eff}}, \quad (17)$$

where the effective tensor has the perfect-fluid form

$$T_{\mu\nu}^{\text{eff}} = (\rho_{\text{eff}} + p_{\text{eff}})u_\mu u_\nu - p_{\text{eff}}g_{\mu\nu}. \quad (18)$$

Matching terms gives

$$\rho_{\text{eff}} = \rho + \frac{\chi}{8\pi}(3\rho - p), \quad (19)$$

$$p_{\text{eff}} = p + \frac{\chi}{8\pi}(3p - \rho). \quad (20)$$

The linear map between (ρ, p) and $(\rho_{\text{eff}}, p_{\text{eff}})$ is invertible for $\chi \neq -4\pi$ and $\chi \neq -2\pi$. Explicitly,

$$\rho + p = \frac{\rho_{\text{eff}} + p_{\text{eff}}}{1 + \chi/(4\pi)}. \quad (21)$$

For practical stellar-structure integration with a physical EoS $p = p(\rho)$, it is useful to write the inverse map explicitly:

$$\rho = \frac{(1 + \frac{3\chi}{8\pi})\rho_{\text{eff}} + \frac{\chi}{8\pi}p_{\text{eff}}}{(1 + \frac{\chi}{4\pi})(1 + \frac{\chi}{2\pi})}, \quad (22)$$

$$p = \frac{\frac{\chi}{8\pi}\rho_{\text{eff}} + (1 + \frac{3\chi}{8\pi})p_{\text{eff}}}{(1 + \frac{\chi}{4\pi})(1 + \frac{\chi}{2\pi})}. \quad (23)$$

These relations ensure a one-to-one closure between the physical EoS and the effective-fluid TOV system whenever the invertibility conditions above are satisfied.

Because the Einstein tensor satisfies the Bianchi identities,

$$\nabla_{\mu}G^{\mu\nu} = 0, \quad (24)$$

the effective tensor is conserved (whereas $T_{\mu\nu}$ is not conserved in general in $f(R, T)$ theories)

$$\nabla_{\mu}T_{\text{eff}}^{\mu\nu} = 0. \quad (25)$$

The theory can be mathematically rewritten as General Relativity sourced by an effective fluid, although the effective thermodynamic variables originate from the matter-geometry coupling and are not independent microphysical fluid variables.

C. Decomposition and Effective Coupling

The field equations can be decomposed as

$$G_{\mu\nu} = (8\pi + 2\chi)T_{\mu\nu} + (2\chi p + \chi T)g_{\mu\nu}. \quad (26)$$

Hence, the coefficient of $T_{\mu\nu}$ may be written as

$$8\pi + 2\chi = 8\pi \left(1 + \frac{\chi}{4\pi}\right). \quad (27)$$

One may define

$$G_{\text{eff}} = G \left(1 + \frac{\chi}{4\pi}\right), \quad (28)$$

but this should be interpreted with care: the extra term $(2\chi p + \chi T)g_{\mu\nu}$ does not vanish in general. Therefore, the model is not equivalent to simply replacing G by G_{eff} in GR; rather, it is GR sourced by an effective fluid, as written in Eq. (17).

D. Modified Tolman-Oppenheimer-Volkoff Equations

We consider the static spherically symmetric metric (signature $+, -, -, -$)

$$ds^2 = e^{\nu(r)}dt^2 - e^{\lambda(r)}dr^2 - r^2d\Omega^2. \quad (29)$$

Defining the mass function by

$$e^{-\lambda(r)} = 1 - \frac{2m(r)}{r}, \quad (30)$$

the tt component of the Einstein equations gives

$$\frac{dm}{dr} = 4\pi r^2 \rho_{\text{eff}}. \quad (31)$$

The rr component yields

$$\nu' = \frac{2(m + 4\pi r^3 \rho_{\text{eff}})}{r(r - 2m)}. \quad (32)$$

From the conservation equation $\nabla_{\mu}T_{\text{eff}}^{\mu\nu} = 0$,

$$\frac{dp_{\text{eff}}}{dr} = -\frac{\nu'}{2}(\rho_{\text{eff}} + p_{\text{eff}}). \quad (33)$$

Substituting ν' we obtain

$$\frac{dp_{\text{eff}}}{dr} = -(\rho_{\text{eff}} + p_{\text{eff}}) \frac{m + 4\pi r^3 \rho_{\text{eff}}}{r(r - 2m)}. \quad (34)$$

Therefore, the effective-fluid stellar-structure system is

$$\frac{dm}{dr} = 4\pi r^2 \rho_{\text{eff}}, \quad (35)$$

$$\frac{dp_{\text{eff}}}{dr} = -(\rho_{\text{eff}} + p_{\text{eff}}) \frac{m + 4\pi r^3 \rho_{\text{eff}}}{r(r - 2m)}. \quad (36)$$

The standard Tolman-Oppenheimer-Volkoff equations [35, 36] are recovered in the limit

$$\chi \rightarrow 0. \quad (37)$$

a. Bridge to the physical pressure gradient: To connect the effective-fluid system to a physical EoS $p = p(\rho)$, we use

$$p_{\text{eff}} = p + \frac{\chi}{8\pi}(3p - \rho), \quad (38)$$

which implies

$$\frac{dp_{\text{eff}}}{dr} = \left(1 + \frac{3\chi}{8\pi}\right) \frac{dp}{dr} - \frac{\chi}{8\pi} \frac{d\rho}{dr}. \quad (39)$$

Hence

$$\frac{dp}{dr} = \frac{1}{1 + \frac{3\chi}{8\pi}} \left[\frac{dp_{\text{eff}}}{dr} + \frac{\chi}{8\pi} \frac{d\rho}{dr} \right]. \quad (40)$$

This equation has the implicit requirement $1 + 3\chi/8\pi \neq 0$, i.e. $\chi \neq -8\pi/3$. This value is already excluded by the dominant-energy-condition branch used for ordinary neutron star matter ($\rho > p$), which gives $\chi \geq -2\pi$, as shown below.

For a barotropic EoS $\rho = \rho(p)$, with $c_s^2 \equiv dp/d\rho$ it becomes,

$$\frac{dp}{dr} = \frac{\frac{dp_{\text{eff}}}{dr}}{\left(1 + \frac{3\chi}{8\pi}\right) - \frac{\chi}{8\pi} \frac{1}{c_s^2}}. \quad (41)$$

To avoid a coordinate singularity in the hydrostatic equation, the denominator of Eq. (41) must not vanish anywhere inside the star. Therefore,

$$\left(1 + \frac{3\chi}{8\pi}\right) - \frac{\chi}{8\pi} \frac{1}{c_s^2} \neq 0, \quad (42)$$

which implies the theoretical constraint

$$\chi \neq -\frac{8\pi}{3 - 1/c_s^2}. \quad (43)$$

For causal matter ($0 < c_s^2 \leq 1$), one also typically requires this factor to remain positive throughout the stellar interior.

E. Constraints on the Coupling Parameter

1. Energy Conditions

Physical solutions require that the effective fluid satisfies

$$\rho_{\text{eff}} > 0, \quad (44)$$

$$\rho_{\text{eff}} + p_{\text{eff}} > 0. \quad (45)$$

Using the definitions above gives the conditions

$$\rho + \frac{\chi}{8\pi}(3\rho - p) > 0, \quad (46)$$

$$\rho + p + \frac{\chi}{4\pi}(\rho + p) > 0. \quad (47)$$

The allowed parameter space of the coupling χ is constrained by three logically distinct requirements: (i) intrinsic theoretical consistency of the effective-fluid formulation, (ii) regularity of the modified hydrostatic equilibrium equations, and (iii) compatibility with astrophysical observations.

Theoretical Constraints

Under the standard neutron star matter assumptions

$$\rho + p > 0, \quad \rho > p, \quad (48)$$

the effective-fluid energy conditions provide intrinsic bounds on χ . From the NEC,

$$(\rho + p) \left(1 + \frac{\chi}{4\pi}\right) > 0 \quad \Rightarrow \quad \chi > -4\pi. \quad (49)$$

From the DEC condition $\rho_{\text{eff}} - p_{\text{eff}} \geq 0$,

$$\rho_{\text{eff}} - p_{\text{eff}} = (\rho - p) \left(1 + \frac{\chi}{2\pi}\right) \geq 0 \quad \Rightarrow \quad \chi \geq -2\pi. \quad (50)$$

For completeness, the SEC gives

$$\rho + 3p + \frac{\chi}{\pi}p > 0 \quad \Rightarrow \quad \chi > -\pi \frac{\rho + 3p}{p} \quad (p > 0), \quad (51)$$

which is model dependent through the local EoS. Therefore, the NEC/DEC bounds are theoretical consistency requirements of the model itself and do not rely on observational data.

2. Regularity and Stability

A second class of constraints follows from hydrostatic regularity of the modified TOV system. From Eq. (41), we define

$$D \equiv \left(1 + \frac{3\chi}{8\pi}\right) - \frac{\chi}{8\pi} \frac{1}{c_s^2}, \quad (52)$$

with the regularity requirement

$$D \neq 0. \quad (53)$$

The corresponding critical sound speed is

$$c_{s,\star}^2 = \frac{\chi}{8\pi + 3\chi}. \quad (54)$$

For realistic neutron star equations of state satisfying $c_s^2 \rightarrow 0$ in the crust, the condition $D \neq 0$ excludes the $\chi > 0$ branch, which generically develops a singularity in dp/dr . On the theoretically consistent neutron star branch (in particular $\chi \geq -2\pi$ from DEC), hydrostatic regularity then selects $\chi < 0$ as the physically viable sector. This regularity/stability constraint is independent of observational data and follows directly from the structure of the modified TOV equations.

3. Astrophysical Constraints

Observational constraints are data driven. Viable configurations must satisfy a maximum mass compatible with heavy-pulsar measurements [1–4], radii consistent

with NICER and GW170817 inferences [5–8, 37], and the GW170817 tidal constraint [37]:

$$M_{\max} \gtrsim 2 M_{\odot}, \quad (55)$$

$$R_{1.4} \sim 11\text{-}14 \text{ km}, \quad (56)$$

$$\Lambda_{1.4} \approx 190_{-120}^{+390}. \quad (57)$$

In practice, multimessenger constraints restrict the magnitude of the coupling to $|\chi| \lesssim \mathcal{O}(0.1)$, although the precise bounds remain mildly dependent on the choice of microscopic equation of state.

a. Synthesis of Constraints The physically viable region is therefore given by the intersection of these domains: theoretical consistency (NEC/DEC), hydrostatic regularity, and multimessenger constraints. In practice, this intersection selects a narrow interval around General Relativity on the negative branch, approximately

$$-\mathcal{O}(0.1) \lesssim \chi < 0. \quad (58)$$

F. Relativistic Enthalpy Formulation

For numerical integrations of neutron star structure it is advantageous to rewrite the Tolman-Oppenheimer-Volkoff (TOV) equations using the relativistic enthalpy as the independent variable [38, 39]. This formulation is widely used in gravitational-wave analyses because it improves numerical stability and works naturally with tabulated equations of state.

Relativistic Enthalpy

For a barotropic equation of state $p = p(\rho)$ the relativistic enthalpy is defined as

$$H(p) = \int_0^p \frac{dp'}{\rho(p') + p'}. \quad (59)$$

Differentiating gives

$$\frac{dH}{dr} = \frac{1}{\rho + p} \frac{dp}{dr}. \quad (60)$$

Substituting the TOV-like equations up to Eq. (41) into the definition of dH/dr yields

$$\frac{dH}{dr} = -\frac{\rho_{\text{eff}} + p_{\text{eff}}}{\rho + p} \frac{1}{\left(1 + \frac{3\chi}{8\pi}\right) - \frac{\chi}{8\pi} \frac{1}{c_s^2}} \frac{m + 4\pi r^3 p_{\text{eff}}}{r(r - 2m)}. \quad (61)$$

Enthalpy Form of the Stellar Structure Equations

It is convenient to use H as the integration variable. Using the identity

$$\frac{d}{dr} = \frac{dH}{dr} \frac{d}{dH}, \quad (62)$$

the stellar structure equations become

$$\frac{dr}{dH} = -\frac{r(r - 2m)}{m + 4\pi r^3 p_{\text{eff}}} \frac{\rho + p}{\rho_{\text{eff}} + p_{\text{eff}}} \left[\left(1 + \frac{3\chi}{8\pi}\right) - \frac{\chi}{8\pi} \frac{1}{c_s^2} \right], \quad (63)$$

$$\frac{dm}{dH} = 4\pi r^2 \rho_{\text{eff}} \frac{dr}{dH}. \quad (64)$$

The integration starts at the stellar center with

$$H = H_c, \quad r = 0, \quad m = 0, \quad (65)$$

and proceeds outward until the surface is reached when $H = 0$ (or equivalently $p = 0$).

Tidal Love Number Equation

The tidal deformability is determined by solving the differential equation governing the metric perturbation function $y(r)$ introduced by Hinderer [40–42]. In the standard radial formulation the equation reads

$$\frac{dy}{dr} = -\frac{y^2}{r} - \frac{y}{r} F(r) - rQ(r), \quad (66)$$

where

$$F(r) = \frac{1 + 4\pi r^2 (p_{\text{eff}} - \rho_{\text{eff}})}{1 - 2m/r}, \quad (67)$$

and

$$Q(r) = \frac{4\pi}{1 - 2m/r} \left(5\rho_{\text{eff}} + 9p_{\text{eff}} + \frac{\rho_{\text{eff}} + p_{\text{eff}}}{c_{s,\text{eff}}^2} \right) - \frac{6}{r^2(1 - 2m/r)} - \frac{4(m + 4\pi r^3 p_{\text{eff}})^2}{r^4(1 - 2m/r)^2}, \quad (68)$$

where the effective sound speed is defined by

$$c_{s,\text{eff}}^2 \equiv \frac{dp_{\text{eff}}}{d\rho_{\text{eff}}} = \frac{c_s^2 + \frac{\chi}{8\pi}(3c_s^2 - 1)}{1 + \frac{\chi}{8\pi}(3 - c_s^2)}. \quad (69)$$

This expression requires

$$1 + \frac{\chi}{8\pi}(3 - c_s^2) \neq 0. \quad (70)$$

During the numerical integration of the tidal perturbation equations, a microscopic tolerance threshold is applied to this denominator to prevent floating-point singularities when evaluating the $Q(r)$ metric potential in the extreme low-density regime.

Tidal perturbation equations follow from the Einstein equations sourced by the effective fluid, the adiabatic sound speed entering the perturbation sector is the effective sound speed rather than the physical sound speed of the microscopic equation of state.

Using the enthalpy variable we obtain

$$\frac{dy}{dH} = \frac{dy}{dr} \frac{dr}{dH}. \quad (71)$$

Thus the full system integrated numerically becomes

$$\frac{dr}{dH} = -\frac{r(r-2m)}{m+4\pi r^3 p_{\text{eff}}} \frac{\rho+p}{\rho_{\text{eff}}+p_{\text{eff}}} \left[\left(1 + \frac{3\chi}{8\pi}\right) - \frac{\chi}{8\pi} \frac{1}{c_s^2} \right], \quad (72)$$

$$\frac{dm}{dH} = 4\pi r^2 \rho_{\text{eff}} \frac{dr}{dH}, \quad (73)$$

$$\frac{dy}{dH} = \left[-\frac{y^2}{r} - \frac{y}{r} F(r) - rQ(r) \right] \frac{dr}{dH}. \quad (74)$$

Because the theory can be written as Einstein gravity sourced by an effective fluid, the perturbation equations governing tidal deformations retain the same structure as in General Relativity, with the physical density and pressure replaced by the effective quantities.

Tidal Deformability

After integrating to the stellar surface $r = R$ we obtain $y_R = y(R)$. The dimensionless tidal Love number is [43, 44]

$$k_2 = \frac{8C^5}{5} (1-2C)^2 \frac{2+2C(y_R-1)-y_R}{\Xi(C, y_R)}, \quad (75)$$

$$\begin{aligned} \Xi(C, y_R) = & 2C [6 - 3y_R + 3C(5y_R - 8)] \\ & + 4C^3 [13 - 11y_R + C(3y_R - 2) \\ & + 2C^2(1 + y_R)] \\ & + 3(1-2C)^2 [2 - y_R + 2C(y_R - 1)] \\ & \times \ln(1-2C). \end{aligned} \quad (76)$$

where $C = M/R$ is the compactness.

The dimensionless tidal deformability measured in gravitational-wave observations is then

$$\Lambda = \frac{2}{3} k_2 C^{-5}. \quad (77)$$

A noteworthy feature of the present model is that the field equations can be written exactly in the form of Einstein gravity sourced by an effective energy–momentum tensor. As a consequence, the linearized perturbation equations governing tidal deformations retain the same structure as in General Relativity. In contrast to other modified gravity theories, such as $f(R)$ gravity [45], no additional dynamical degrees of freedom appear in the perturbation sector. The modification of the tidal response therefore enters only through the effective thermodynamic variables and through the effective sound speed $c_{s,\text{eff}}^2 = dp_{\text{eff}}/d\rho_{\text{eff}}$.

IV. EFFECTIVE EQUATION OF STATE AND STIFFENING MECHANISM

In the numerical analysis, we employ realistic EoSs that support maximum masses near $2M_\odot$ and are broadly consistent with merger tidal constraints [1, 2, 9, 37]. We therefore consider APR4, SLY, WFF1, and MPA1.

To understand the impact of the $f(R, T) = R + 2\chi T$ modification on stellar structure, we examine how the physical fluid variables map into their effective counterparts, which are the quantities that source the gravitational field. In this theory, the geometric modification acts as an additional contribution to the energy-momentum tensor, leading to an effective energy density ρ_{eff} and an effective pressure p_{eff} , given in Eqs. (19) and (20).

In Fig. 1, we compare the physical EoS (GR baseline, $\chi = 0$) with the effective EoS for the MPA1 model, in units of MeV/fm³. For negative values of the coupling constant χ , the effective pressure p_{eff} is systematically higher than the physical pressure p at fixed energy density ρ . This shift constitutes an effective “stiffening” mechanism. Because the effective EoS is stiffer than the physical one, the configuration can withstand stronger gravitational compression before reaching the stability limit.

Figure 2 shows that this effect is model-independent. Across all considered equations of state, ranging from soft models like APR4 to stiffer models like MPA1, the presence of a negative χ consistently shifts the curve upward.

V. MASS-RADIUS AND OBSERVATIONAL CONSTRAINTS

In this section we present numerical solutions of the modified Tolman-Oppenheimer-Volkoff (TOV) and tidal

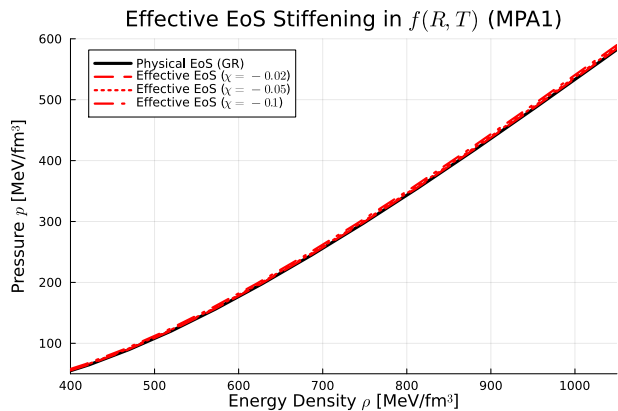


FIG. 1. Effective EoS stiffening for the MPA1 model for different coupling strengths. All units are in MeV/fm^3 .

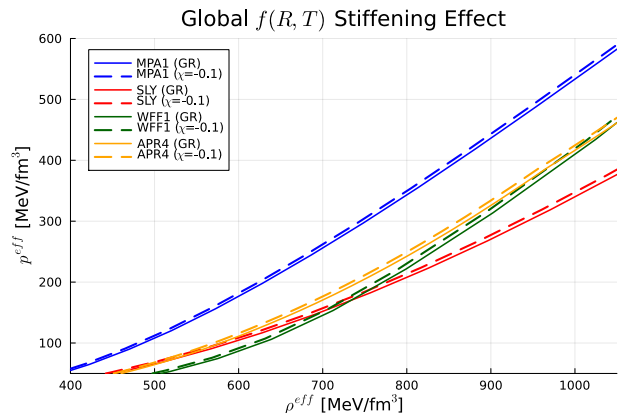


FIG. 2. Global stiffening effect across various nuclear models (MPA1, SLY, WFF1, APR4), comparing GR to $\chi = -0.1$. All units are in MeV/fm^3 .

equations in $f(R, T) = R + 2\chi T$ gravity. We compare the predictions for APR4, SLY, WFF1, and MPA1 with multimessenger constraints from massive pulsars, NICER radius measurements (PSR J0030+0451 and PSR J0740+6620), and GW170817.

A. Mass-Radius Relations and the Crustal Sound Speed Effect

Figures 3, 4, 5, and 6 display the mass-radius ($M - R$) relations for the selected EoSs. The black solid lines represent the General Relativity (GR) baseline ($\chi = 0.0$), while the dashed, dotted, and dash-dotted lines represent increasing strengths of the modified gravity coupling ($\chi = -0.02, -0.05$, and -0.1 , respectively).

As χ becomes more negative, the effective stiffening of the EoS (as discussed in Section IV) manifests as an outward shift in the stellar radius and a modest increase in the maximum mass. However, a critical phenomenon arises when applying extended gravity

theories to realistic neutron star models that include a proper crust, as first demonstrated by Lobato et al. [46].

A trend that is also evident in Figs. 3-6 is that the separation between curves with different χ is typically more pronounced in the low-mass region than near the maximum-mass branch. In other words, the coupling constant leaves a stronger imprint on less massive stars. Physically, these stars have lower compactness and a larger relative contribution from the outer layers, where the EoS is softer and the $1/c_s^2$ factor amplifies the geometric correction terms. For very massive stars, the stiff high-density core and stronger relativistic compactness partially reduce the relative impact of changing χ on global observables such as the radius.

In the modified hydrostatic equilibrium equations, the geometric correction factor exhibits a strict dependence on the inverse square of the fluid's sound speed, $c_s^2 = dp/d\rho$. Deep in the stellar core, the matter is highly incompressible, c_s^2 is large, and the modified gravity terms remain well-behaved. However, as the integration reaches the stellar crust, the density drops precipitously, and the EoS becomes extremely soft ($c_s^2 \rightarrow 0$). Lobato et al. showed that this $1/c_s^2$ dependence forces the $f(R, T)$ contributions to explode in the low-density regime, artificially inflating the crust.

Our current numerical integrations corroborate this finding. If the coupling constant χ is not strictly bounded (e.g., $|\chi| \leq 0.02$) or if the sound speed is not regularized in the extreme vacuum, the stellar envelope undergoes unphysical runaway inflation, blowing the radius out to over 30 km. To ensure stable numerical integration through the outermost stellar layers and avoid solver stalling as $c_s^2 \rightarrow 0$, we introduce a minimum numerical floor for the sound speed strictly within the geometric correction factor. Specifically, the evaluation of the $f(R, T)$ modification assumes an effective minimum bound of $c_s^2 \geq 0.015$ in the extreme-vacuum limit. This regularization isolates the unphysical runaway inflation of the crust while preserving the exact hydrostatic dynamics throughout the dense stellar interior. Consequently, because realistic stellar structures demand a crust, the overall maximum mass increase is severely tempered compared to older, simplistic “bare star” models. The inclusion of the crust dictates that $f(R, T)$ gravity cannot arbitrarily raise the mass limit of soft EoS models without concurrently destabilizing the stellar surface.

Taken together, Figs. 3-6 reveal a clear hierarchy. SLY offers the best overall compromise with the current radius bands for mild negative couplings. APR4 remains comparatively viable but lies near the compact edge of the allowed region, whereas WFF1 is more marginal because it stays systematically on the low-radius side of the NICER-favored range. By contrast, MPA1 is the most strongly constrained: negative χ shifts it toward larger radii and, when combined with its large deformabilities, quickly drives it into tension with multimessenger bounds. This pattern supports the

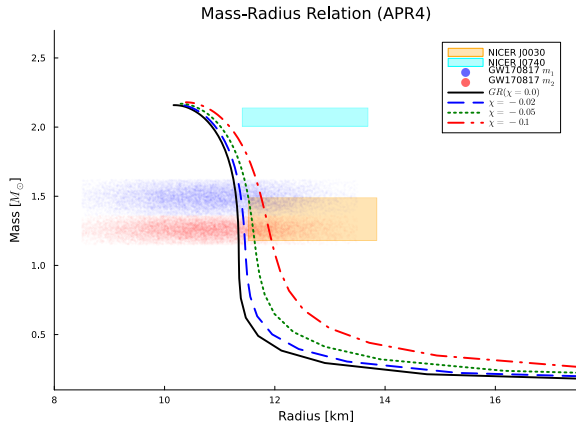


FIG. 3. Mass-radius relation for the APR4 equation of state. The shaded rectangular regions denote the 1σ NICER constraints for PSR J0030+0451 (orange) and PSR J0740+6620 (cyan), while the background clouds represent the 90% credible intervals for the primary and secondary masses from GW170817.

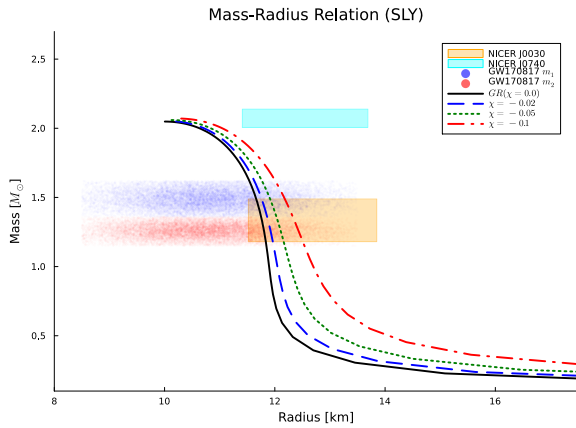


FIG. 4. Mass-radius relation for the SLY equation of state. The plotting conventions are the same as in Fig. 3.

interpretation that modified-gravity stiffening competes with observational constraints from both sides of parameter space: overly compact branches remain too small, whereas very stiff branches become too extended and too deformable.

B. Single Star Tidal Deformability

The internal stiffness of the star is directly probed by its tidal deformability, $\Lambda = (2/3)k_2C^{-5}$, where k_2 is the Love number and $C = M/R$ is the compactness. Figure 7 summarizes $\Lambda(M)$ for APR4, SLY, WFF1, and MPA1.

Figure 7 shows that, for all EoSs, more negative χ shifts the $\Lambda(M)$ sequences upward, as expected from

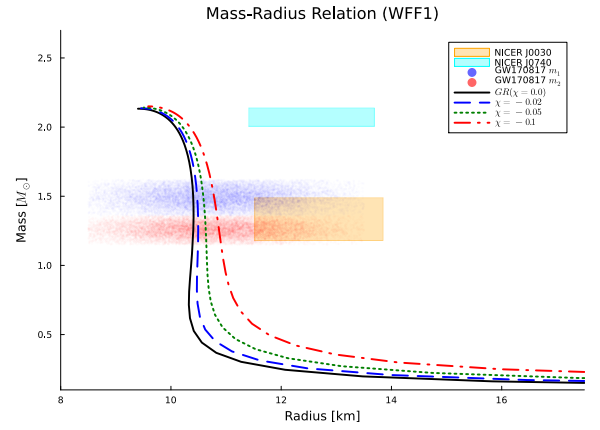


FIG. 5. Mass-radius relation for the WFF1 equation of state. The plotting conventions are the same as in Fig. 3.

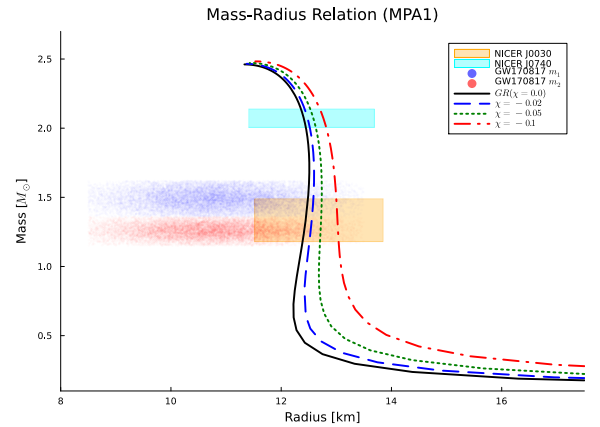


FIG. 6. Mass-radius relation for the MPA1 equation of state. The stronger rightward shift for negative χ highlights the tension of very stiff models with multimessenger radius and tidal constraints.

the larger radii and smaller compactness. The black marker with error bar at $1.4M_\odot$ denotes the GW170817 reference value $\Lambda_{1.4} = 190^{+390}_{-120}$ and provides a direct visual discriminator among models.

The figure also reveals a clear hierarchy: MPA1 yields the largest deformabilities and WFF1 the smallest, while APR4 and SLY remain intermediate and partially overlap over much of the mass range. Consequently, the stiffer models come into stronger tension with tidal constraints as χ decreases, whereas the softer-to-intermediate cases remain compatible over a broader range of mild negative couplings.

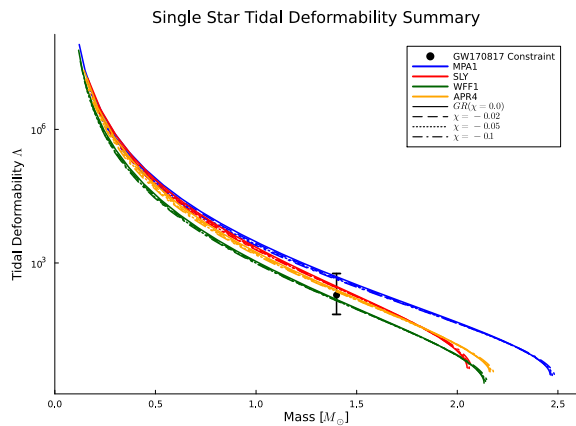


FIG. 7. Dimensionless tidal deformability Λ as a function of stellar mass for APR4, SLY, WFF1, and MPA1. The black marker with error bar corresponds to the GW170817-inspired reference constraint at $1.4 M_{\odot}$.

C. Binary Tidal Deformability

To evaluate the theory against the LIGO/Virgo multimessenger data, we plot the binary tidal deformability (Λ_1 vs. Λ_2) in Fig. 8. The gray cloud represents the synthetic 90% credible posterior for GW170817, assuming a chirp mass of $\mathcal{M} = 1.188 M_{\odot}$ and a mass ratio $q \in [0.73, 1.0]$.

The trajectories in the Λ_1 - Λ_2 plane provide a stringent consistency test. APR4 and SLY pass through the densest part of the GW170817 posterior for mild couplings, WFF1 traces the lower-deformability edge of the allowed region, and MPA1 is shifted toward larger deformabilities. As χ becomes more negative (from solid to dash-dotted curves), the tracks move upward and to the right, progressively reducing the overlap with the observationally favored region.

This binary phase space encapsulates the main tension of $f(R, T)$ gravity in neutron stars: negative values of χ can help soft EoSs raise the maximum mass to the $2.0 M_{\odot}$ level required by heavy pulsars, but overly negative values also drive the binary tidal deformability beyond the GW170817 credible region. Combined with the crustal sound-speed limitations highlighted by [46], this leaves only a narrow viable interval for the coupling constant and confirms that departures from General Relativity in the dense-matter regime must remain small.

VI. CONCLUSIONS

In this work, we formulated and tested a conservative $f(R, T)$ model in which the modified field equations are written as Einstein equations sourced by an effective fluid. This construction keeps the gravitational sector independent of the microscopic equation of state and

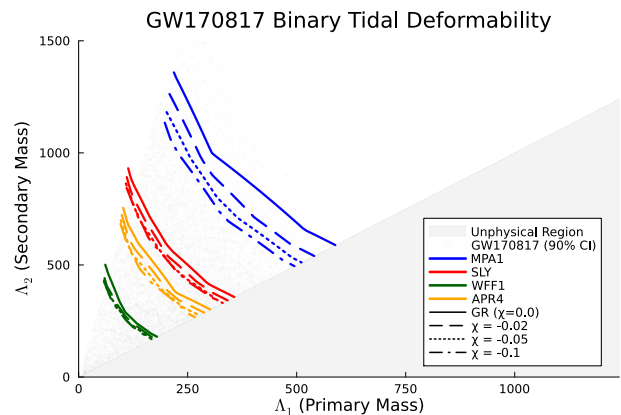


FIG. 8. Binary tidal deformability (Λ_1 vs. Λ_2) for the studied EoSs. The colored lines trace the EoS trajectories mapped across the adopted GW170817 mass-ratio domain. The line styles indicate the strength of the $f(R, T)$ modification. The shaded gray region represents the unphysical domain ($\Lambda_2 < \Lambda_1$), while the scatter cloud serves as a proxy for the official LIGO/Virgo 90% credible posterior.

avoids reconstructing the action from a chosen EoS. Within this framework, we derived the stellar-structure and tidal-perturbation equations in enthalpy form and solved them for realistic hadronic EoSs.

Our results show that negative values of the coupling constant χ effectively stiffen stellar matter, shifting the mass-radius and tidal-deformability curves upward. This effect is not uniform along the stellar sequence: it is strongest for low-mass stars, where lower compactness and a larger relative crust contribution amplify the modified-gravity corrections. Near the maximum-mass branch, the stiff high-density core reduces the relative impact of χ on global observables.

At the same time, the crustal regime is central to the viability bounds. Because the modified equilibrium equations contain terms proportional to $1/c_s^2$, the low-density region can trigger strong amplification and unphysical radius inflation if $|\chi|$ is too large. When this effect is treated consistently with realistic crusts, the allowed parameter space is significantly reduced. Confronting the model with multimessenger constraints from massive pulsars, NICER radii, and GW170817 tidal bounds, we find that only small departures from GR remain viable, with couplings close to zero and typically limited to mild negative values. Among the realistic EoSs considered here, SLY provides the best overall compromise with current multimessenger bounds for mild negative couplings; APR4 remains viable but tends to lie on the compact side of the allowed region; WFF1 is more marginal because its radii remain systematically small; and MPA1 is the most strongly constrained because the modified-gravity stiffening quickly pushes it toward both larger radii and larger tidal deformabilities.

A central conclusion is therefore methodological: realistic equations of state are indispensable for testing

modified gravity with neutron stars. As emphasized by modern nuclear-matter compilations and constraints [26], only EoSs that consistently describe core and crust microphysics can provide reliable bounds on gravity parameters. Otherwise, simplified or overly idealized EoSs can either hide or exaggerate the gravity signal, worsening the gravity-microphysics degeneracy [47]. Our results reinforce that robust constraints on $f(R, T)$ models require realistic tabulated EoSs and full multimessenger consistency checks.

These conclusions are consistent with, and extend, the findings of our previous analysis in Ref. [46], where the crust/sound-speed pathology in realistic $f(R, T)$ neutron star models was first highlighted. Compared with the conservative study of Ref. [24], the key methodological difference is that their analysis focused on hydrostatic equilibrium and asteroseismology using polytropic equations of state, which are useful for trend exploration but limited for direct multimessenger inference.

A key physical implication of the present work is that this difference is not merely methodological; it changes the stability conclusions decisively. Polytropic toy models without a realistic crust effectively remove the low-density regime in which c_s^2 becomes very small. In our formulation, the modified hydrostatic terms scale as $1/c_s^2$; therefore, once realistic crust physics is included and $c_s^2 \rightarrow 0$, the geometric corrections can grow catastrophically, driving unphysical envelope

inflation and eliminating acceptable equilibrium solutions unless $|\chi|$ is minute. Accordingly, stability diagnostics inferred only from radial-oscillation spectra or binding-energy cusps computed with crust-free polytropes are not physically complete for realistic $f(R, T)$ neutron stars, because they miss this dominant crust-driven destabilization channel.

Our results show that, once realistic tabulated EoSs and crust physics are included, the viable coupling interval becomes narrower and the systematics clearer. The present study advances this line of work by recasting the theory in a conservative effective-tensor form and by combining mass-radius, single-star $\Lambda(M)$, and binary (Λ_1, Λ_2) diagnostics in a unified multimessenger analysis. Overall, the evidence indicates that any viable $f(R, T)$ effect in neutron stars must be perturbative around General Relativity.

Acknowledgments

RVL was supported by INCT-FNA (Instituto Nacional de Ciência e Tecnologia, Física Nuclear e Aplicações), research Project No. 464898/2014-5, and acknowledges support from CAPES/CNPq. GAC would like to thank CNPq, Fundação de Amparo a Pesquisa do Espírito Santo and Fundação Araucária for financial support under processes #314121/2023-4, PROFIX 12/2024 and NAPI “Fenômenos extremos no Universo”.

-
- [1] P. B. Demorest, T. Pennucci, S. M. Ransom, M. S. E. Roberts, and J. W. T. Hessels, *Nature* **467**, 1081 (2010), 1010.5788.
- [2] J. Antoniadis, P. C. C. Freire, N. Wex, T. M. Tauris, R. S. Lynch, M. H. van Kerkwijk, M. Kramer, C. Bassa, V. S. Dhillon, T. Driebe, J. W. T. Hessels, V. M. Kaspi, V. I. Kondratiev, N. Langer, T. R. Marsh, M. A. McLaughlin, T. T. Pennucci, S. M. Ransom, I. H. Stairs, J. van Leeuwen, J. P. W. Verbiest, and D. G. Whelan, *Science* **340**, 6131 (2013), 1304.6875.
- [3] H. T. Cromartie, E. Fonseca, S. M. Ransom, P. B. Demorest, Z. Arzoumanian, H. Blumer, P. R. Brook, S. Burke-Spolaor, S. J. Chamberlin, S. Chatterjee, J. M. Cordes, R. D. Ferdman, W. Fiore, N. Garver-Daniels, P. A. Gentile, J. W. T. Hessels, G. Jones, M. T. Lam, D. R. Lorimer, R. S. Lynch, M. A. McLaughlin, T. T. Pennucci, I. H. Stairs, K. Stovall, J. Swiggum, and W. W. Zhu, *Nature Astronomy* **4**, 72 (2020), 1904.06759.
- [4] E. Fonseca, H. T. Cromartie, T. T. Pennucci, P. S. Ray, A. Y. Kirichenko, S. M. Ransom, P. B. Demorest, I. H. Stairs, Z. Arzoumanian, H. Blumer, P. R. Brook, S. Burke-Spolaor, S. Chatterjee, J. M. Cordes, T. Enoto, W. Fiore, P. A. Gentile, D. C. Good, J. L. Han, J. W. T. Hessels, R. J. Jennings, G. Jones, M. T. Lam, T. J. W. Lazio, D. R. Lorimer, R. S. Lynch, M. A. McLaughlin, C. Ng, J. Olson, R. Spiewak, K. Stovall, J. Swiggum, and W. W. Zhu, *The Astrophysical Journal Letters* **915**, L12 (2021), 2104.00880.
- [5] T. E. Riley, A. L. Watts, S. Bogdanov, P. S. Ray, R. M. Ludlam, S. Guillot, Z. Arzoumanian, C. L. Baker, A. V. Bilous, D. Chakrabarty, K. C. Gendreau, A. K. Harding, W. C. G. Ho, J. M. Lattimer, S. M. Morsink, and T. E. Strohmayer, *The Astrophysical Journal* **887**, L21 (2019), 1912.05702.
- [6] M. C. Miller, F. K. Lamb, A. J. Dittmann, S. Bogdanov, Z. Arzoumanian, K. C. Gendreau, S. Guillot, A. K. Harding, W. C. G. Ho, J. M. Lattimer, R. M. Ludlam, S. Mahmoodifar, S. M. Morsink, P. S. Ray, T. E. Strohmayer, K. S. Wood, T. Enoto, R. Foster, T. Okajima, G. Prigozhin, and Y. Soong, *The Astrophysical Journal* **887**, L24 (2019), 1912.05705.
- [7] T. E. Riley, A. L. Watts, P. S. Ray, S. Bogdanov, S. Guillot, S. M. Morsink, A. V. Bilous, Z. Arzoumanian, D. Choudhury, J. S. Deneva, K. C. Gendreau, A. K. Harding, W. C. G. Ho, J. M. Lattimer, M. Loewenstein, R. M. Ludlam, C. B. Markwardt, T. Okajima, C. Prescod-Weinstein, R. A. Remillard, M. T. Wolff, E. Fonseca, H. T. Cromartie, M. Kerr, T. T. Pennucci, A. Parthasarathy, S. Ransom, I. Stairs, L. Guillemot, and I. Cognard, *The Astrophysical Journal Letters* **918**, L27 (2021), 2105.06980.
- [8] M. C. Miller, F. K. Lamb, A. J. Dittmann, S. Bogdanov, Z. Arzoumanian, K. C. Gendreau, S. Guillot, W. C. G. Ho, J. M. Lattimer, M. Loewenstein, S. M. Morsink, P. S. Ray, M. T. Wolff, C. L. Baker, T. Cazeau, S. Manthripragada, C. B. Markwardt, T. Okajima,

- S. Pollard, I. Cognard, H. T. Cromartie, E. Fonseca, L. Guillemot, M. Kerr, A. Parthasarathy, T. T. Pennucci, S. Ransom, and I. Stairs, *The Astrophysical Journal Letters* **918**, L28 (2021), 2105.06979.
- [9] B. Abbott, R. Abbott, T. D. Abbott, *et al.* (LIGO Scientific, Virgo), *Phys. Rev. Lett.* **119**, 161101 (2017), 1710.05832.
- [10] T. P. Sotiriou and V. Faraoni, *Reviews of Modern Physics* **82**, 451 (2010), 0805.1726.
- [11] A. De Felice and S. Tsujikawa, *Living Reviews in Relativity* **13**, 3 (2010), 1002.4928.
- [12] S. Nojiri and S. D. Odintsov, *Physics Reports* **505**, 59 (2011), 1011.0544.
- [13] S. S. Yazadjiev, D. D. Doneva, and K. D. Kokkotas, *Phys. Rev. D* **91**, 084018 (2015), 1501.04591.
- [14] K. V. Staykov, D. D. Doneva, S. S. Yazadjiev, and K. D. Kokkotas, *Journal of Cosmology and Astroparticle Physics* **10** (10), 006, 1407.2180.
- [15] S. Capozziello, M. De Laurentis, R. Farinelli, and S. D. Odintsov, *Phys. Rev. D* **93**, 023501 (2016), 1509.04163.
- [16] A. V. Astashenok, S. Capozziello, S. D. Odintsov, and V. K. Oikonomou, *Phys. Lett. B* **816**, 136222 (2021), 2103.04144.
- [17] A. V. Astashenok, S. Capozziello, S. D. Odintsov, and V. K. Oikonomou, *Europhysics Letters* **136**, 59001 (2022), 2111.14179.
- [18] T. Harko, F. S. N. Lobo, S. Nojiri, and S. D. Odintsov, *Physical Review D* **84**, 024020 (2011), 1104.2669.
- [19] R. V. Lobato *et al.*, *The European Physical Journal Plus* **134**, 132 (2019), 1803.08630.
- [20] Z. Yousaf, K. Bamba, and M. Z.-u.-H. Bhatti, *Phys. Rev. D* **93**, 124048 (2016), 1606.00147.
- [21] J. Barrientos O. and G. F. Rubilar, *Phys. Rev. D* **90**, 028501 (2014).
- [22] S. Chakraborty, *General Relativity and Gravitation* **45**, 2039 (2013), 1212.3050.
- [23] S. I. dos Santos, G. A. Carvalho, P. H. R. S. Moraes, C. H. Lenzi, and M. Malheiro, *Eur. Phys. J. Plus* **134**, 398 (2019), 1803.07719.
- [24] J. M. Pretel, S. E. Jorás, R. R. Reis, and J. D. Arbañil, *Journal of Cosmology and Astroparticle Physics* **08** (08), 055, 2105.07573.
- [25] G. A. Carvalho, S. I. Dos Santos, P. H. R. S. Moraes, and M. Malheiro, *Int. J. Mod. Phys. D* **29**, 2050075 (2020), 1911.02484.
- [26] M. Oertel, M. Hempel, T. Klähn, and S. Typel, *Reviews of Modern Physics* **89**, 015007 (2017), 1610.03361.
- [27] P. Bedaque and A. W. Steiner, *Physical Review Letters* **114**, 031103 (2015), 1408.5116.
- [28] S. Altiparmak, C. Ecker, and L. Rezzolla, *Astrophys. J. Lett.* **939**, L34 (2022), 2203.14974.
- [29] X.-T. He, F. J. Fattoyev, B.-A. Li, and W. G. Newton, *Physical Review C* **91**, 015810 (2015), 1408.0857.
- [30] M. Minamitsuji and H. O. Silva, *Physical Review D* **93**, 124041 (2016), 1604.07742.
- [31] K. Yagi and N. Yunes, *Phys. Rept.* **681**, 1 (2017), 1608.02582.
- [32] D. D. Doneva *et al.*, *Physical Review D* **108**, 044054 (2023).
- [33] H. O. Silva, in *Recent Progress on Gravity Tests: Challenges and Future Perspectives*, edited by C. Bambi and A. Cárdenas-Avendaño (Singapore, 2024) pp. 101–147, 2407.17578.
- [34] S. Typel, M. Oertel, and T. Klähn, *Phys. Part. Nucl.* **46**, 633 (2015), arXiv:1307.5715.
- [35] R. C. Tolman, *Physical Review* **55**, 364 (1939).
- [36] J. R. Oppenheimer and G. M. Volkoff, *Physical Review* **55**, 374 (1939).
- [37] The LIGO Scientific Collaboration and the Virgo Collaboration, *Physical Review Letters* **121**, 161101 (2018), 1805.11581.
- [38] L. Lindblom, *The Astrophysical Journal* **398**, 569 (1992).
- [39] L. Lindblom, *Physical Review D* **82**, 103011 (2010), 1009.0738.
- [40] T. Hinderer, *The Astrophysical Journal* **677**, 1216 (2008), 0711.2420.
- [41] T. Hinderer, B. D. Lackey, R. N. Lang, and J. S. Read, *Physical Review D* **81**, 123016 (2010), 0911.3535.
- [42] S. Postnikov, M. Prakash, and J. M. Lattimer, *Physical Review D* **82**, 024016 (2010), 1004.5098.
- [43] T. Binnington and E. Poisson, *Physical Review D* **80**, 084018 (2009), 0906.1366.
- [44] T. Damour and A. Nagar, *Physical Review D* **80**, 084035 (2009).
- [45] S. S. Yazadjiev, D. D. Doneva, and K. D. Kokkotas, *The European Physical Journal C* **78**, 818 (2018), 1803.09534.
- [46] R. Lobato, O. Lourenço, P. H. R. S. Moraes, C. H. Lenzi, M. de Avellar, W. de Paula, M. Dutra, and M. Malheiro, *Journal of Cosmology and Astroparticle Physics* **12** (12), 039, 2009.04696.
- [47] P. H. R. S. Moraes, J. D. V. Arbañil, and M. Malheiro, *Journal of Cosmology and Astroparticle Physics* **06** (06), 005, 1511.06282.